observations suggest that thiamin pyrophosphokinase activity is responsible for the regional distribution of thiamin content, thiamin influx and thiamin pyrophosphate turnover in rat brain. In relation to the thiamin transport, our preliminary experiments showed that thiamin uptake into rat brain synaptosomes was inhibited by pyrithiamin, an inhibitor of thiamin pyrophosphokinase, and it did not show a saturability with respect to external thiamin concentration (data not shown). Furthermore, the thiamin uptake into cerebellar synaptosomes was higher than that into cortical synaptosomes (data not shown). These findings suggest that the thiamin uptake occurs by a facilitated diffusion in which thiamin pyrophosphokinase activity is involved. In view of the recent finding[18] that a thiamin pyrophosphate binding protein is present in the soluble fraction, the possibility is that a soluble thiamin binding protein might exist as a carrier for thiamin transport and its complex with thiamin would be the actual substrate for the thiamin pyrophosphate synthesis. If so, thiamin pyrophosphokinase activity would be directly coupled to the transport system for thiamin. Obviously further studies are required.

1 Johnson, L. R., and Gubler, C. J., Biochim. biophys. Acta *156* (1968) 85.
2 Wakabayashi, A., Iwashima, A., and Nose, Y., Biochim. biophys. Acta *429* (1976) 1087.
3 Peterson, J. W., Gubler, C. J., and Kuby, S. A., Biochim. biophys. Acta *397* (1975) 377.
4 Wakabayashi, Y., Vitamins (in Japanese) *52* (1978) 223.
5 Wakabayashi, Y., Vitamins (in Japanese) *52* (1978) 229.
6 Nose, Y., Iwashima, A., and Nishimura, H., in: Thiamine, p. 157. Eds C. J. Gubler, M. Fujiwara and P. M. Dreyfus. John Wiley and Sons, New York 1976.
7 Rindi, G., and Ventura, U., Experientia *23* (1967) 175.
8 Ventura, U., Ferrari, G., Tagliabue, R., and Rindi, G., Life Sci. *8* (1969) 699.
9 Ferrari, G., Ventura, U., and Rindi, G., Life Sci. *10* (1971) 67.
10 Komai, T., and Shindo, H., J. Vitam. *18* (1972) 55.
11 Komai, T., Kawai, K., and Shindo, H., J. Nutr. Sci. Vitam. *20* (1974) 163.
12 Rindi, G., Patrini, C., Comincioli, V., and Reggiani, C., Brain Res. *181* (1980) 369.
13 Rindi, G., Comincioli, V., Reggiani, C., and Patrini, C., Brain Res. *293* (1984) 329.
14 Glowinski, J., and Iversen, L. L., J. Neurochem. *13* (1966) 655.
15 Deus, B., in: Methods in Enzymology, vol. 18A, p. 221. Eds D. B. McCormick and L. D. Wright. Academic Press, New York 1970.
16 Sen, I., and Cooper, J. R., Neurochem. Res. *1* (1976) 65.
17 Lowry, O. H., Rosebrough, N. J., Farr, A. L., and Randall, R. J., J. biol. Chem. *193* (1951) 265.
18 Nishino, K., Itokawa, Y., Nishino, N., Piros, K., and Cooper, J. R., J. biol. Chem. *258* (1983) 11871.

0014-4754/85/070924-02$1.50 + 0.20/0

α-Particle track autoradiographic study of the distribution of a [^{211}At]-astatinated drug in normal tissues of the mouse

J. S. Mitchell, I. Brown and R. N. Carpenter

University of Cambridge School of Clinical Medicine, Research Laboratories, Radiotherapeutic Centre, Addenbrooke's Hospital, Hills Road, Cambridge CB2 2QQ (England), 25 May 1984

Summary. The microscopic distribution of the potential endoradiotherapeutic drug, 6-[^{211}At]-astato-2-methyl-1,4-naphthoquinol bis (diphosphate salt) in normal tissues of the mouse has been studied by α-particle track autoradiography. The uptake into critical radiosensitive tissues, especially bone marrow, colon and lung, was low.
Key words. Mouse; endoradiotherapy; α-particle track autoradiography; 6-[^{211}At]-astato-2-methyl-1,4-naphthoquinol bis (diphosphate salt).

This is an account of an autoradiographic study of the distribution of the potential α-emitting endoradiotherapeutic drug, 6-[^{211}At]-astato-2-methyl-1,4-naphthoquinol bis (diphosphate salt), abbreviated 6-[^{211}At]-astato-MNDP (fig. 1), in normal tissues of the mouse. Preliminary results of this development for experiments in mice with a transplanted chemically induced adenocarcinoma of the rectum are described[2]. Since then, the results of therapeutic experiments in mice have been reported[3-5].

Materials and methods. Astatine is the highest member of Group VIIB in the Periodic Table. It has only radioactive isotopes and the most suitable of these, $^{211}_{85}$At, has a radioactive half-life 7.21 h. The ranges of the α-particles of ^{211}At in unit density tissue are either 55 μm corresponding to energy 5.87 MeV for 42% of the disintegrations or 80 μm corresponding to energy 7.45 MeV for approximately 58% of the disintegrations. ^{211}At was prepared by the nuclear reaction ^{209}Bi(α, 2n) ^{211}At in the Nuffield 1.52 m cyclotron at Birmingham University, U.K., using a 28 MeV external α-particle beam. The compound 6-[^{211}At]-astato-MNDP was synthesized initially via a chloromercuri-intermediary[6] but more recently by an in vacuo heterogeneous isotopic exchange process with 6-iodo-MNDP[7]. The final astatinated product was purified by ion-exchange chromatography; 6-[^{211}At]-astato-MNDP was not carrier-free; its specific activity was approximately 50 μCi/mmole (6-iodo-MNDP). The resulting solution of 6-[^{211}At]-astato-MNDP was buffered to pH 7.4 and then sterilized by membrane filtration (Millipore 0.22 μm) for injection. Dose aliquots were determined by measurement of the 77–92 keV ^{211}Po K (K-L, M, N) X-rays using a 2 in NaI (TL) well crystal.

Male C57BL mice, of weight 25–30 g, bearing a single 0.5–0.8 g transplanted CMT-93 rectal adenocarcinoma[8] in the flank, were used in this study. 1 h prior to the injection of 6-[^{211}At]-astato-MNDP, mice received a s.c. injection of potassium perchlorate (10 mg kg^{-1}) in order to block thyroid function, and so prevent the uptake of any free ^{211}At. Animals received a single i.p. injec-

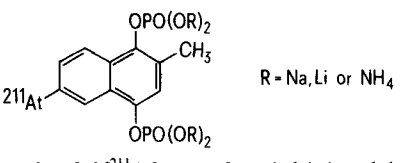

Figure 1. Formula of 6-[^{211}At]-astato-2-methyl-1,4-naphthoquinol bis (diphosphate salt), abbreviated 6-[^{211}At]-astato-MNDP.

Distribution of origins of α-particle tracks in cells of normal tissues in mice with transplanted adenocarcinoma of rectum after single i.p. injection of compound 6-^{211}At-astato-MNDP, with thyroid blocking with $KClO_4$

Normal tissue	Time and dose	Counts of track origins and number of cells (also as percentage)	Cells of track origin	Percentage or fraction of track origins in nucleus including nuclear membrane	Assessment of uptake of compound in tissue
Colon	30 min after 200 kBq (5.4 μCi)	45/ca 375,000 cells (0.0120 ± 0.0018%)	Acinar cells (31/41, 76%) Smooth muscle cells (10/41, 24%)	58% (18/31)	Very low
	3 h after 740 kBq (20 μCi)	7/1271 cells (0.55 ± 0.21%)	Acini		Low
	6 h after 1.85 MBq (50 μCi)	0/1159 cells	Acini		Very low
		12/1167 cells (1.03 ± 0.30%)	Stained area excluding acini	5/12	Small but definite
	12 h after 3.77 MBq (101.8 μCi)	28/1083 cells (2.59 ± 0.48%)	Acini	64% (18/28)	Definite (no muscle seen in these section)
Femoral bone marrow	30 min after 200 kBq (5.4 μCi)	1 track in 15 sections	Probably a myeloblast		Extremely low
	3 h after 740 kBq (20 μCi)	10/1379 cells (0.73 ± 0.23%)		9/12	Low
	6 h after 1.85 MBq (50 μCi)	10/808 cells (1.24 ± 0.39%)		7/10	Definite though relatively low
	12 h after 3.77 MBq (101.8 μCi)	26/1242 cells (2.09 ± 0.41%)		54% (14/26)	Definite
Liver	30 min after 200 kBq (5.4 μCi)	48/3103 cells (1.55 ± 0.22%)	Hepatocytes (90/104, 86.5%) R.E. and Kuppfer cells (14/104, 13.5%)	94% (45/48)	Definite
	3 h after 740 kBq (20 μCi)	24/1171 cells (2.05 ± 0.41%)	Hepatocytes	8/24	Definite
	12 h after 3.77 MBq (101.8 μCi)	43/1286 cells (3.34 ± 0.50%)	Hepatocytes	69.8% (30/43)	Definite
Spleen	30 min after 200 kBq (5.4 μCi)	Malpighian bodies: 67/1897 cells (3.53 ± 0.42%)		81.5% (53/65)	Definite
		Pulp: 5/1112 cells (0.45 ± 0.20%)			
	6 h after 1.85 MBq (50 μCi)	Pulp: 5/1420 cells (0.35 ± 0.16%) (most of sections lost)			Low (very few tracks none dense)
	12 h after 3.77 MBq (101.8 μCi)	Malpighian bodies: 87/1048 cells (8.30 ± 0.86%)			High
		Pulp: 10/1124 cells (0.89 ± 0.28%)			Relatively low
Lung	30 min after 200 kBq (5.4 μCi)	Lung, including a respiratory bronchiole 13/1188 cells (1.09 ± 0.30%)	Type II pneumocytes (alveolar cells)	54% (7/13)	Low
	3 h after 740 kBq (20 μCi)	Expanded lung: 8/1136 cells (0.70 ± 0.25%)	Type II pneumocytes (alveolar cells)	5/8	Low
	6 h after 1.58 MBq (50 μCi)	Expanded lung: 53/1116 cells (4.75 ± 0.64%)	Type II pneumocytes (alveolar cells)	51% (27/53)	Relatively high
		Dense area adjacent to respiratory bronchiole: 74/1590 cells (4.65 ± 0.53%)	Type II pneumocytes (alveolar cells)	70% (50/74)	Substantially the same as expanded lung

Continued

Normal tissue	Time and dose	Counts of track origins and number of cells (also as percentage)	Cells of track origin	Percentage or fraction of track origins in nucleus including nuclear membrane	Assessment of uptake of compound in tissue
		Area of solid lung: 33/605 cells (5.45 ± 0.92%)			Possible error in cell counts
	12 h after 3.77 MBq (101.8 μCi)	Expanded lung: 71/1105 cells (6.43 ± 0.74%)	Type II pneumocytes (alveolar cells)	37% (26/71)	Relatively high
Testis	3 h after 740 kBq (20 μCi)				Very few long tracks
	6 h after 1.85 MBq (50 μCi)	3/329 cells (0.9%)	Spermatogonia		No long dense tracks but some fine tracks with ⩾ 10 small grains
	12 h after 3.77 MBq (101.8 μCi)	56/1285 (4.36 ± 0.57%)	Spermatogonia Interstitial tissue	79% (37/47) 7/9	Definite

tion of 6-[^{211}At]-astato-MNDP (74 kBq–3.77 MBq [2–102 μCi]), and were sacrificed, using ether, at intervals over 12 h.

Autoradiography was carried out on frozen sections of tissues of thickness about 3 μm, prepared in a cryostat with freeze-dehydration to minimize the diffusion of radioactivity. Sections were then transferred to microscope slides and coated with 1:1 diluted warmed liquid Ilford Emulsion K2 or K0 to give final thickness of the emulsion layer about 2.5 or 5 μm. Exposures were from 15 to 24 h at 2 °C. The sections were fixed histologically in 1:3 v/v acetic-alcohol for 10 min.

After photographic development and the use of a 1% acetic acid stop bath, the slides were dipped in 0.5% gelatin solution, in order to deep the sections stuck on the slide, with subsequent drying in air. This was then followed by photographic fixation and washing. The slides were then transferred to acetate buffer of pH 4.2 and stained with methyl green/pyronin mixture in 1% solution for 30 min at room temperature[9]. In these experiments, the emulsion density was found to be 1.5–2.5 g/ml.

Control experiments were carried out both in the absence of radioactivity and on sections after the completion of α-decay. A detailed histopathological examination was undertaken on all tissue specimens.

As far as possible, all the cells in tissue sections were examined for α-particle tracks; at least 10 grains were required to define a track. α-particle tracks were counted in specific areas, using a defined grid-system. Cellular photomicrography was also carried out concomitantly.

Parallel bio-distribution studies have been carried out by measurement of the radioactivity of macroscopic specimens[10].

Aspects of the physical behavior of α-particle tracks in nuclear emulsions, within the context of the problem of quantitative autoradiographic analysis, have been fully discussed in connection with the uptake and intracellular distribution of 6-[^{211}At]-astato-MNDP in tumor tissue[4].

Results and discussion. The cellular, intracellular and temporally related distribution of the origins of α-particle tracks emanating from 6-[^{211}At]-astato-MNDP or its active metabolite(s) in normal tissues from tumor-bearing mice is shown in the table. Examples of autoradiographs of frozen sections of normal tissues of mice 30 min after i.p. injection of 200 kBq (5.4 μCi) of the compound, 6-[^{211}At]-astato-MNDP are shown in figure 2. Parallel histological studies provided supporting evidence for the identification of the cells.

These results are consistent with the biodistribution studies[10] and give a more detailed picture of the distribution of the compound in different cells and tissues, including the proportion of track origins in the nucleus and nuclear membrane.

The most striking findings are the very low levels of uptake in the normal colon and bone marrow. They are supported by the

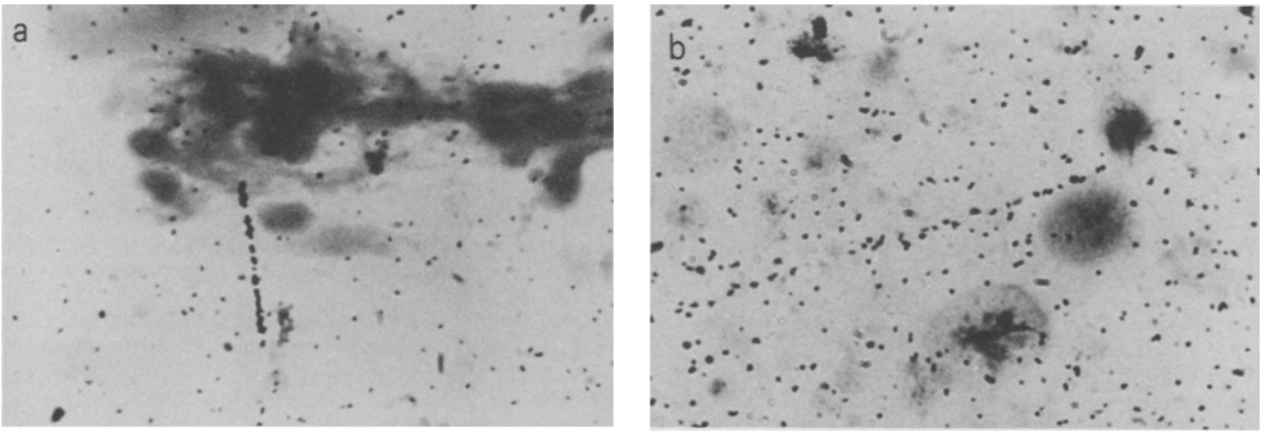

Figure 2. Autoradiographs of sections of some normal tissues of mice after i.p. injection of therapeutic doses of 6-[^{211}At]-astato-MNDP. × 1600. *a* Lung: shows the origin of the α-particle in the nuclear membrane of a cell; probably a pneumocyte Type II, in a partially collapsed area. *b* Spleen: shows the origin of the α-particle in plasma membrane of a cell of splenic pulp; probably a reticular cell.

qualitative results of the autoradiographs with tritiated MNDP for normal human tissues[11-13].

Conclusion. α-Particle track autoradiography provides a useful method for evaluating the detailed localization of the compound in cells and tissues. The uptake into critical tissues such as bone marrow, colon and lung was low.

These results are important from the point of view of the development of this endoradiotherapeutic drug.

1 Acknowledgments. We are grateful to Prof. J. Walker and the staff of the Radiation Centre and Nuffield Cyclotron, Department of Physics, Birmingham University, England, and for the cooperation of Dr A. T. M. Vaughan, Department of Immunology, The Medical School, Birmingham. We are also grateful to Dr L. M. Franks of the Imperial Cancer Research Fund Laboratories, Lincoln's Inn Fields, London, for the supply of the original mouse tumors. We also thank Mr L. F. H. Beard and Mr M. Johns and the staff of the Department of Medical Illustration and Photography, Addenbrooke's Hospital, Hills Road, Cambridge.

2 Mitchell, J. S., Brown, I., and Carpenter, R. N., Experientia *39* (1983) 337.
3 Mitchell, J. S., Brown, I., and Carpenter, R. N., in: Essays on Human Alkaline Phosphatase. Eds T. Stigbrand and W. H. Fishman. Alan R. Liss, Inc., New York 1984.
4 Mitchell, J. S., Brown, I., and Carpenter, R. N., Br. J. Radiol., prepared for publication (1984).
5 Brown, I., Carpenter, R. N., and Mitchell, J. S., Br. J. Radiol., prepared for publication (1984).
6 Brown, I., Int. J. appl. Radiat. Isotop. *13* (1982) 7.
7 Brown, I., Radiochem. radioanalyt. Lett. *53* (1982) 343.
8 Franks, L. M., and Hemmings, G. T., J. Path. *124* (1978) 35.
9 Rogers, A. N., in: Techniques of Autoradiography, chapter 8, p. 153. Elsevier/North Holland. Biomedical Press, Amsterdam 1979.
10 Brown, I., Carpenter, R. N., and Mitchell, J. S., Int. J. appl. Radiat. Isotop. *35* (1984) 843.
11 Mitchell, J. S., Strahlentherapie *127* (1965) 497.
12 Mitchell, J. S., Clin. Radiol. *16* (1965) 305.
13 Mitchell, J. S., Cancer if curable, why not cured? W. Heffer and Sons Ltd, Cambridge 1971.

0014-4754/85/070925-04$1.50 + 0.20/0

Transfer of oligosaccharide from oligosaccharide pyrophosphoryl dolichol to endogenous acceptor proteins in human breast malignant and normal tissues

A. R. Santa Cruz and A. Baldi

Instituto de Biología y Medicina Experimental, Obligado 2490, 1428 Buenos Aires (Argentina), 18 May 1984

Summary. We have prepared dolichylpyrophosphoryl-[^{14}C]-oligosaccharide (Dol-PP-oligosaccharide) from calf thyroid. Microsomal fractions from human breast tissues catalyzed the transfer of labeled oligosaccharide to endogenous acceptor proteins. Malignant tumors showed higher activity of the oligosaccharide transferring enzyme than normal tissue. With kojibiose (Kj), and inhibitor of (Glc_3)-glucosidase, an increase in the radioactivity associated with glycoprotein was observed.

Key words. Oligosaccharide transfer; human breast cancer glycoproteins; kojibiose.

The fact that glycosylation of eucaryotic proteins involves lipid-linked saccharides as intermediates is well documented[1,2]. The final step in this metabolic pathway is the transfer 'en bloc' of the oligosaccharide from Dol-PP-$(GlcNAc)_2Man_9Glc_3$ to an asparagine residue of a protein acceptor.

We have already demonstrated the conversion of GDP-Man and UDP-Glc to Dol-P-Man and Dol-P-Glc respectively, catalyzed by the microsomal fraction from human breast tissues[3,4]. In addition, differences were detected between normal, benign and neoplastic samples[5].

Due to the present interest in glycoproteins as possible biological markers in human breast neoplasia[6-8] we extended our studies to the reaction involving the membrane-bound oligosaccharide transferring enzyme.

Materials and methods. Chemicals and substrates. All organic solvents were analytic grade. [^{14}C]-Glc (360 μCi/μmol) was from New England Nuclear. Kojibiose was supplied by Koch Light. All culture media were from GIBCO Laboratories. The hen oviduct Dol-PP-oligosaccharide, heterogeneous, consisting of four species with the composition $Glc_{0-2}Man_9GlcNAc_2$ and Glc_3- as a major component, used in the experiments described in tables 1 and 2, was kindly supplied by Dr Quesada.

Preparation of [^{14}C]-oligosaccharide-lipid. Calf thyroid slices (4 g) were incubated as described by Spiro et al.[9] with 250 μCi of [^{14}C]-Glc for 3 h at 37 °C. The tissue was washed 3 times with 0.25 M sucrose and homogenized in 0.2 M EDTA, pH 7.7. Chloroform and methanol were then added to achieve a mixture of chloroform/methanol/water (C/M/W) 3:2:1. To obtain the oligosaccharide-lipid, the interphase pellet was extracted as described by Spiro et al.[9].

Preparation of human breast microsomal fraction. Human breast tissues, obtained from mastectomy specimens or biopsies, were classified as benign or malignant according to their anatomopathological characteristics. The 'normal' sample was peritumoral tissue from the same patient. The tissues were homogenized as described[3]. Two types of membrane preparations were used. 'Unwashed' membranes were prepared as previously described[3], and 'washed' membranes according to Lucas et al.[10], omitting the incubation treatment.

Assay for transfer of labeled oligosaccharide from oligosaccharide-lipid to endogenous acceptor proteins. Standard reaction mixtures contained radiolabeled oligosaccharide-lipid ($6-10 \times 10^3$ cpm), 100 mM Tris-HCl pH 7.5, 8 mM $MgCl_2$, 8 mM $MnCl_2$, 2 mM EDTA, 40 mM 2-S-ethanol, 0.2% Triton X-100, with or without 1 mM Kj. The reactions were initiated by adding 350–500 μg of microsomal protein to the incubation mixture to a final volume of 50 μl, and incubated at 15 °C for 5–15 min. The reaction was stopped with 1 ml of C/M 3:2 and processed as described[3]. The 'lower phase' of the Folch's partition contains the lipid-bound monosaccharides and oligosaccharides up to 7–8 hexoses[11], while sugars are in the 'upper phase'. The extract C/M/W 10:10:3 contains polyprenyl-PP-oligosaccharides with more than seven hexoses[12] and the 'hot TCA resistant' material is considered as glycoprotein[13].

Other methods. Mild acid hydrolysis, radioactivity and protein determination, paper chromatography and microanalytic DEAE-cellulose chromatography used here were previously described[3].

Results and discussion. In our previous studies[3,4] the procedure used to assess protein glycosylation was based on the transfer of Man or Glc from GDP-[^{14}C]-Man or UDP-[^{14}C]-Glc respectively, to the endogenous protein fraction. In these studies the optimum temperature for glucoprotein formation was 15 °C[3].

Based on this observation we incubated microsomes from malignant and benign human breast tumors with labeled hen oviduct Dol-PP-oligosaccharide at 15 °C. Table 1 shows negligible radio-